JTTEE5 8:545-552
©ASM International

Peer Reviewed

Plasma Spraying Using Ar-He-H_2 Gas Mixtures

S. Janisson, A. Vardelle, J.F. Coudert, E. Meillot, B. Pateyron, and P. Fauchais

(Submitted 7 October 1998; in revised form 25 May 1999)

In plasma spraying, the properties of the plasma-forming gas largely control the characteristics of the plasma jet and the momentum, heat, and mass transfers to the particles injected in the flow. The objective of this work was to investigate the effect of gas composition on the static and dynamic behaviors of the plasma jet. The latter behaviors were investigated from measurements of arc voltage and plasma jet velocity. Ternary gas mixtures of argon, helium, and hydrogen were used. The results were expressed as correlations between arc voltage and flow velocity, and the operating parameters of the gun for a specific nozzle diameter.

Keywords arc voltage fluctuations, Ar-He-H_2 gas mixtures, gas thermodynamic and transport properties, inert plasma spraying, plasma jet velocity

1. Introduction

Plasma spraying is commonly carried out using a mixture of two gases: the primary gas, argon (Ar), and the secondary gas, hydrogen (H) or helium (He). The composition of the plasma-forming gas influences (a) the formation of the plasma jet and the arc behavior inside the anode nozzle, (b) the mixing of the plasma jet with the enveloping atmosphere, and (c) the acceleration and heating of the particles injected in the flow.

Argon ensures arc stabilization inside the nozzle and controls the transport rate of mass and the momentum of the flow. Argon is characterized by a high mass, a rather high viscosity (2.7×10^{-4} kg/m · s at 10,000 K), and a relatively low thermal conductivity (0.6 W/m · K at 10,000 K).

Helium and hydrogen increase the energy capacity of the gun. They also enhance the heat transfer to particles, which occurs mainly by conduction through the boundary layer surrounding particles, as they have a high thermal conductivity. The latter is higher for hydrogen than it is for helium: 3.7 W/m · K and 2.4 W/m · K respectively at 10,000 K. In addition, helium has a high viscosity, especially above 10,000 K (3.1×10^{-4} kg/m · s at 10,000 K and 4.3×10^{-4} kg/m · s at 15,000 K), due to its higher ionization potential of 24.6 eV compared to 15.7 eV for argon and 13.6 eV for hydrogen. When the temperature increases beyond room temperature, the values of viscosity are controlled first by the interactions between neutral molecules (for diatomic molecules). Then, as dissociation starts, viscosity values are controlled by neutral atoms; at even higher temperatures, the charged particles control the values. In reality, when ionization occurs, the viscosity decreases with increasing temperature. The drop in viscosity is due to the ionization of the gas, resulting in a Coulomb force of relatively long range between particles. For helium, this decrease is not observed below 17,000 K due to the higher ionization potential of helium (Ref 1).

S. Janisson and **E. Meillot,** CEA/DAM Le Ripault, BP 16, 37260 Monts, France; and **A. Vardelle, J.F. Coudert, B. Pateyron,** and **P. Fauchais,** SPCTS, University of Limoges, 123 avenue A. Thomas, 87060 Limoges cedex, France. Contact e-mail: armelle@ensil.unilim.fr.

In a plasma spray process, the composition of the plasma gas is one of the operating parameters that can help to increase the deposition efficiency and possibly the lifetime of electrodes. The mixing of argon with both hydrogen and helium makes it possible to combine the advantages of the high thermal conductivity of hydrogen and the high viscosity of helium. Previous studies have shown that such ternary gas mixtures were favorable to the spraying of ceramics, resulting in a significant increase in deposition efficiency and giving rise to the development by Air Liquide of the ternary plasma-forming gas mixture "Spral" (Ref 2).

The present study deals with ternary gas mixtures of argon, helium, and hydrogen for a large range of gun operating conditions.

Nomenclature

D	Internal nozzle diameter, m
G	Mass flow rate of the plasma gas, kg/s
h^*	Mass enthalpy of the plasma gas at T^*, J/kg
I	Arc current, A
k	Thermal conductivity of the plasma gas, W/m · K
k^*	Thermal conductivity of the plasma gas at T^*, W/m · K
Pr	Prandtl number, $Pr = \frac{\mu^* \times h^*}{k^* \times T^*}$
q_c	Conductive flux to particle $q_c = \frac{1}{R_p} \times \int_{T_p}^{T_\infty} k(T)dT$, W/m^2
Re	Reynolds number, $\mathrm{Re} = \frac{G}{\mu^* \times D}$
R_p	Radius of the particle, m
Si	Energy number (second number of Yas'ko), $Si = \frac{I^2}{\sigma^* \times h^* \times G \times D}$
T_p	Particle surface temperature, K
T_∞	Undisturbed plasma temperature, K
T^*	Temperature for which electron concentration in the plasma is higher than 1 vol%, K
V	Arc voltage, V
v_{max}	Maximum gas velocity at 2 mm downstream the nozzle exit, m/s
μ^*	Viscosity of the plasma gas at T^*, kg/m · s
ρ^*	Specific density of the plasma gas at T^*, kg/m^3
σ^*	Electrical conductivity of the plasma gas, $(\Omega \cdot \mathrm{m})^{-1}$

The first objective of this work was to determine the domain of gun parameters for which the gun is stable. This analysis was made by studying the dynamic behavior of the plasma jet. The second objective was to establish correlations between the time-average arc voltage and the jet velocity, and the variables of the spray process. Such correlations allow a reduction in the number of experiments in the investigated domain. Moreover, they can assist in developing a model for the on-line control of the process.

2. Thermodynamic and Transport Properties of Ternary Gas Mixtures

The volume percentage of argon in the gas mixture was varied between 30 and 50 vol%, the percentage of hydrogen between 7.4 and 25, and the percentage of helium between 30 and 55.6. The thermodynamic and transport properties (Ref 1) of the different mixtures were computed using the ADEP software (University of Limoges and CNRS, Limoges, France, 1986) (Ref 3). Figures 1 to 4 represent the specific enthalpy and the transport properties of the various gas mixtures at atmospheric pressure. The compositions of these mixtures and their molecular weights are given in Table 1.

The variations in enthalpy are mainly due to the heat of dissociation of H_2 and the ionization of the various gases, Ar, He, and H_2. This effect is noticeable for low percentages of H_2 because the dissociation of hydrogen starts at a rather low temperature (3000 K). The maximum dissociation is found at about 3800 K at atmospheric pressure. The energy of ionization of helium is higher than that of argon (24.5 eV compared to 15.7 eV), and the addition of helium modifies the enthalpy of the mixture above 17,000 K and at volume percentages higher than 60.

For a constant gas flow rate, an increase in H_2 and/or He content results in an increase in the specific enthalpy of the mixture. This is due to the decrease of the gas mass resulting from the lowering of argon content. A rough estimate from the curves of Fig. 1 shows that, at 20,000 K, the gas enthalpy increases by ~23% when the argon content decreases by 20%.

Because of its high dissociation and ionization peaks, H_2 shows the highest value of thermal conductivity, whereas Ar has the lowest value (Ref 1). An increase of the relative H_2 content thus implies an improvement in the thermal conductivity for ternary mixtures, especially at low temperature (T > 3500 K) (Fig. 2). Increasing the amount of He in the gas mixtures also improves the thermal conductivity in a smaller range than the thermal conductivity with H_2 at temperatures higher than 10,000 K. As a result, thermal conductivity is mainly controlled by the percentage of H_2 up to 5000 K and by both percentages of H_2 and He at temperatures above this level.

In thermal plasma jets, heat transfer to particles injected in the flow occurs mainly by conduction through the boundary layer. If kinetic equilibrium prevails in this boundary layer, the rate of heat transfer, q_c, through the gas shell can be expressed as (Ref 4):

$$q_c = \frac{1}{R_p} \times \int_{T_p}^{T_\infty} k(T)dT \qquad \text{(Eq 1)}$$

where R_p is the radius of the particle, k the thermal conductivity of the gas, T_p is the particle surface temperature, and T_∞ is the undisturbed plasma temperature. The heat flux, of course, follows the same trend as the gas thermal conductivity. Adding H_2 to the mixture results in an increase as soon as the temperature exceeds 4000 K (Fig. 3).

The viscosities of the ternary mixtures as a function of temperature are shown in Fig. 4. These viscosities are very close to that of pure argon up to 11,000 K. Above this temperature, the viscosity decreases and exhibits some variation between the various mixtures. First, the interactions between the neutral species control the values of viscosity. After the first ionization of Ar and H, the viscosity decreases. This can be explained by the relatively long-range Coulomb forces between charged particles, resulting in a decrease in their mobility when the density increases. The decrease in mobility causes an increase in the collision integrals for charged particles.

The differences in the curves, above 11,000 K, are explained by the helium content in the mixture; the higher the helium content is, the higher the gas mixture viscosity, due to the higher ionization potential of He.

3. Arc Behavior and Plasma Jet Dynamics

In plasma spray guns, the arc voltage is characterized by fluctuations at frequencies ranging from approximately 2 to 20 kHz. These arise from the continuous movement of the arc root attachment spot on the anode (resulting from the interactions of electromagnetic, thermal, and dynamic phenomena in the arc column) and the anode attachment region (Ref 5, 6). This effect results in a continuous fluctuation of the length and diameter of the plasma jet at the exit of the torch. Moreover, the mixing of the free jet with the quiescent ambient jet induces turbulent phenomena that are governed by large density and velocity differences between the plasma jet and the surrounding gas. Large-scale ed-

Table 1 Plasma spraying conditions

Gas mixture, vol%			Molecular weight,	Total gas flow rate,		Arc current,		
Ar	He	H_2	g/mol	slm		A		
50	40	10	21.7	27	50	320	460	600
50	30	20	21.4	27	50	320	460	600
40	50	10	18.1	27	50	320	460	600
40	40	20	17.8	27	50	320	460	600
37	55.6	7.4	17.1	27	50	320	460	600
30	45	25	14.3	…	50	320	460	600

dies extend from the outer edge of the shear layer toward the jet center in which they are broken down into smaller eddies and mixed with the flow (Ref 7). This phenomenon is enhanced by the fluctuations of the jet originating from the arc root motion.

As the time constant of the arc fluctuations is in the order of the residence time of the particles within the plasma jet, the arc behavior can be affected by these fluctuations. The arc behavior can be investigated from the time dependence of the arc voltage and from transient measurements of the plasma light in the potential core, where the entrained fluid has not yet penetrated. Further downstream in the flow, such measurements will depend more on the flow turbulence.

4. Experimental Procedure

4.1 Spraying Conditions

Experiments were carried out using a F4 plasma gun (Sulzer-Metco, Wohlen, Switzerland) with a 6 mm nozzle diameter and a vortex injection of the plasma-forming gas in the arc zone. They were conducted in argon atmosphere at 10^5 Pa chamber pressure. The chamber was equipped with two 18.5×3.5 mm glass windows for optical diagnostics and could be moved in a vertical plane according to two orthogonal directions, so that the optical axis for measurement was fixed. The various sets of spray conditions are listed in Table 1.

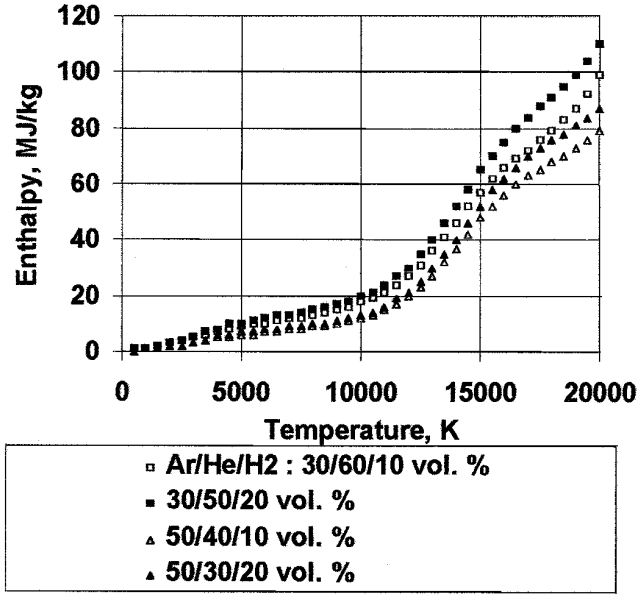

Fig. 1 Temperature dependence of the enthalpy of the Ar/He/H_2 gas mixtures

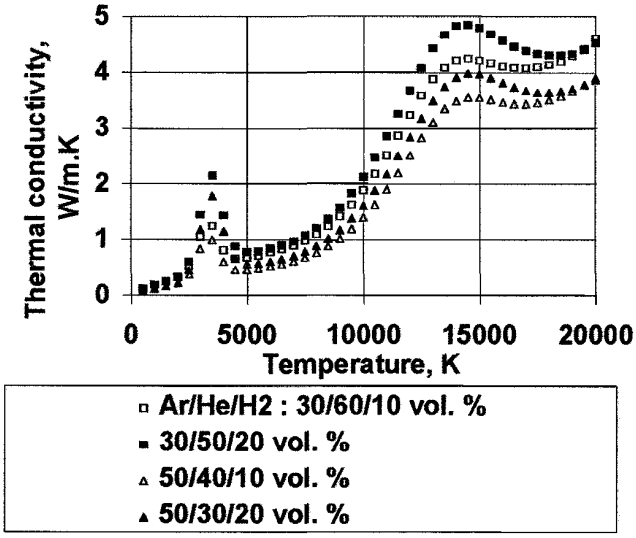

Fig. 2 Temperature dependence of the thermal conductivity of Ar/He/H_2 gas mixtures

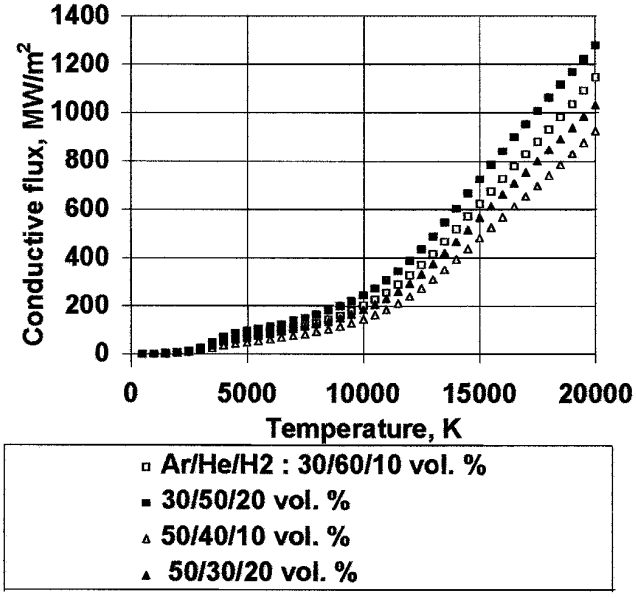

Fig. 3 Temperature dependence of the conductive heat flux to a 40 μm particle for various Ar/He/H_2 gas mixtures

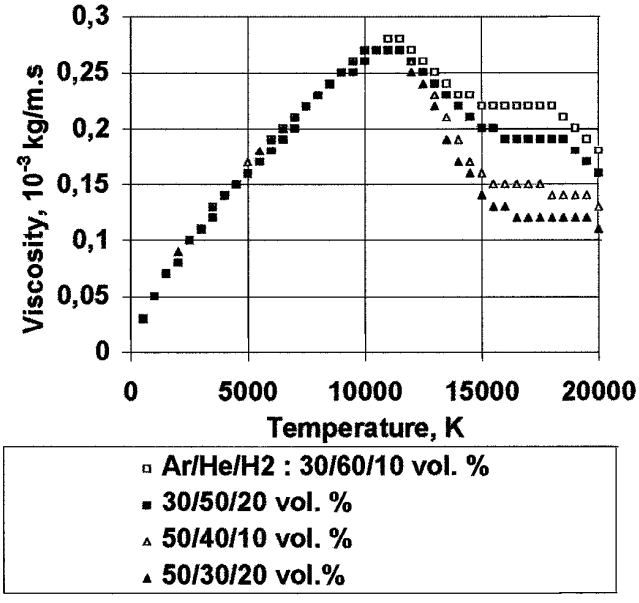

Fig. 4 Temperature dependence of the viscosity of Ar/He/H_2 gas mixtures

Peer Reviewed

The process parameters investigated in this study were (a) composition of the gas mixture, (b) total gas flow rate, and (c) arc current intensity. The volume content of hydrogen was set to 7.4, 10, 20, or 25%, while the content of helium was fixed to 30, 40, 45, 50, or 55.6%. Indeed, if the flow characteristics are modified as soon as hydrogen is mixed with argon, the helium content must be at least equal to 30% to significantly affect these characteristics.

4.2 Gas Flow Velocity Measurements

In the potential core, the plasma jet velocity was determined from the light fluctuations, which originate in the arc root instabilities (Ref 5). These fluctuations are supposed to propagate at the flow velocity. The measurement method is closely connected to a time-of-flight method. It consisted in determining the delay between two light signals collected at two locations that were 10 mm apart in the plasma jet.

A diagram of the experimental setup is shown in Fig. 5. An image of the plasma jet was formed through a lens and a beam splitter on the end of two optical fibers 100 μm in diameter. The latter guided the collected light toward two photomultipliers connected with a dual-track digitizing oscilloscope operating at a sampling rate of 10 μs/point. The location of the tips of both fibers was accurately known from a mechanical device involving two orthogonal microdisplacement systems. The accuracy on the distance between the two sampling points was 0.2%.

The data processing consisted in determining the time delay between both tracks registered by the oscilloscope. A cross-correlation procedure involving the first 256 points of each track was used. These points were selected from a smooth-edged time window. The temporal resolution was determined by the number of points per track used for the cross-correlation process (256), the sampling rate (10 μs/point), and, to a lesser extent, the shape of the time window. Each of the measured velocities, therefore, corresponded to a mean value that was time-averaged over 2 ms; in other words, the velocimetry method was limited to the velocity-fluctuating components in the 0 to 500 Hz frequency range.

In addition, from a single recording associated with a single location in the jet, a temporal evolution of the velocity was obtained over the period for data collection of approximately 80 ms. The time-evolution of arc voltage was recorded with a sampling rate of 10 μs per point.

Previous experimental work (Ref 8, 9) carried out using this method for plasma jet velocity measurement has shown that it

Table 2 Arc voltage and gas velocity for a total gas flow rate of 27 slm

		First measurement		Second measurement	
Ar/He/H_2 mixture, vol%	Arc current, A	Voltage, *V*	Velocity at the center of jet, m/s	Voltage, *V*	Velocity at the center of jet, m/s
50/40/10	600	30 ± 0.1	802 ± 96	37.1 ± 0.9	1602 ± 575
50/40/10	460	31 ± 0.5	729 ± 126	37.3 ± 0.3	912 ± 228
40/50/10	600	30.5 ± 0.1	864 ± 67	37.5 ± 0.5	1301 ± 268
40/50/10	460	35.5 ± 0.9	916 ± 328	39.5 ± 0.5	1587 ± 232

Note: Gas velocity was measured on the torch centerline, 2 mm downstream of the nozzle exit.

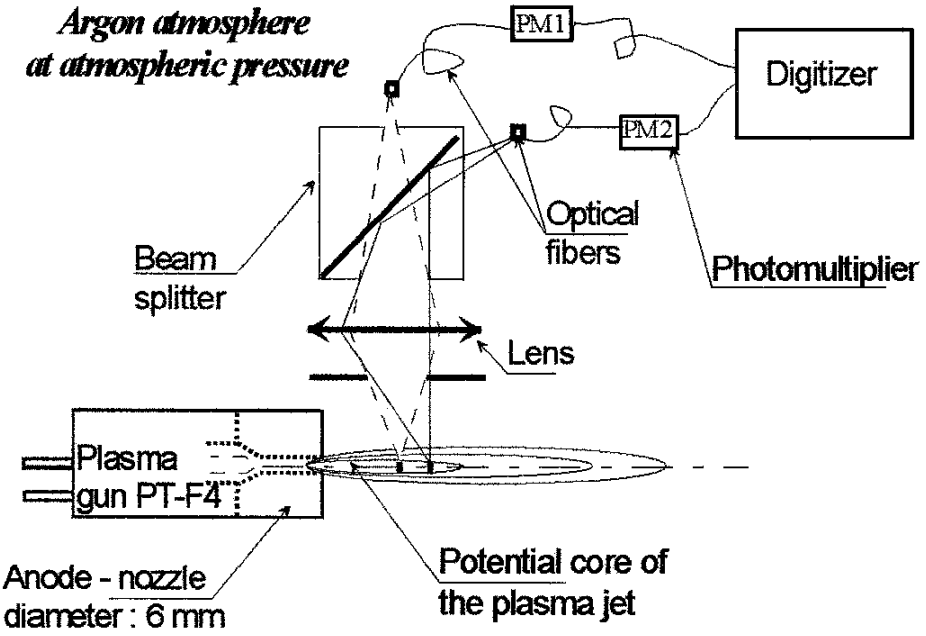

Fig. 5 Schematic view of the experimental setup for gas velocity measurements

can be confidently applied in the potential core of the jet where mixing with the surrounding gas has not begun.

5. Dynamic Behavior of the Plasma Jet

The average values and standard deviations of arc voltage and gas velocity at the nozzle exit (2 mm) were measured, at different times, for the various sets of the spray conditions given in Table 1.

The scatter of both variables for every run, and between separate runs, showed that the spraying conditions used in the present study resulted in two operating modes for the gun. Mode 1 was stable and characterized by a low time-dependence of the average values of voltage and gas velocity. Moreover, the radial profile of gas velocity were quasi-symmetrical with a parabolic shape. Mode 2 was unstable and characterized by a high level of fluctuations. The scatter between separate measurements was large, and the radial velocity profiles were asymmetrical.

The latter mode was only observed for the low total flow rate of 27 slm when the arc current was high (460 or 600 A), the helium content was high (40 or 50%), and the hydrogen content was low (10%). Table 2 lists the four torch operating conditions giving rise to this mode and shows examples of arc voltage and gas velocity variations at two different instants.

This unstable mode is largely due to the low gas-flow rate of argon (ranging between 10 and 13 slm), which is not high enough to stabilize the arc. In addition, the vortex injection of the plasma-forming gas, which was assumed to help the constriction of the arc column, was ineffective when the gas flow rate was too low. It should be noticed that the measurements of voltage and gas velocity carried out with a longitudinal injection of gas along the cathode showed more stable plasma jets, even with the critical conditions.

In fact, the mass flow rate has a complex role on the arc behavior because it determines the rate at which the arc is stretched and lengthened. The mass flow rate also largely controls the turbulence and the perturbation in the fringes of the arc column.

Previous experiments have shown that an increase in the mass flow rate causes a significant increase in the voltage amplitude fluctuations and a decrease in the lifetime of the arc attachment point at one location (Ref 5, 10). In the present study, the levels of voltage fluctuation were similar for total gas flow rate of 27 and 50 slm, as a result of the unstable torch operation at 27 slm.

Table 3 shows the fluctuations of the arc voltage and plasma velocity for the different spraying conditions. Both fluctuations are defined as the ratio of the standard deviation of the variable to the average value.

The motion of the arc attachment spot on the anode is mainly governed by the thickness and stability of the "colder" gas layer surrounding the arc column. The thicker this layer is, the higher the voltage amplitude fluctuations and the lower the frequency characteristic of arc root motion (Ref 11). On the contrary, when the cold gas layer surrounding the arc column is thin, any perturbation in the column fringes gives rise to arc breakdown and rearcing. In the latter condition, the arc generally has not enough

Table 3 Fluctuations of arc voltage and gas velocity for the various plasma spraying conditions

Gas mixture composition Ar/He/H_2, vol%	Total gas flow rate, slm	Arc current, A	Arc voltage fluctuation, %	Gas velocity fluctuation, %
50/40/10	27	320	1.4	28.3
		460	0.7	32.0
		600	1.9	35.9
	50	320	1.3	18.3
		460	2.5	18.6
		600	3.1	26.5
50/30/20	27	320	1.0	6.3
		460	0.6	11.9
		600	1.2	18.1
	50	320	1.1	14.7
		460	1.3	17.7
		600	1.2	18.8
40/50/10	27	320	2.1	11.9
		460	1.3	14.6
		600	1.5	20.6
	50	320	1.2	13.2
		460	1.4	14.5
		600	1.8	20.3
40/40/20	27	320	0.5	10.9
		460	1.5	22.2
		600	1.2	24.8
	50	320	0.5	28.3
		460	0.8	14.9
		600	0.9	41.4
37/55.6/7.4	27	320	1.0	15.2
		460	1.2	21.8
		600	2.4	10.5
	50	320	1.0	9.2
		460	1.5	15.0
		600	1.7	18.5

time to be significantly lengthened under the intricate action of gas flow and electromagnetic forces. Therefore, voltage fluctuations are generally lower. The thickness of the cold gas layer can be reduced by increasing the energy input to the arc or decreasing the gas flow rate, as long as it is high enough to ensure the constriction of the arc column.

Increasing the percentage of hydrogen increases the electric field of the arc and constricts and lengthens the arc column. This effect can be enhanced by a demixing phenomenon within the arc column, which causes a higher density of hydrogen in periphery of the column (Ref 12). As well, increasing the helium content improves the plasma jet stability because of a slightly better constriction of the arc column and a reduction in the turbulence of the flow.

6. Static Behavior of the Plasma Jet

The behavior of the plasma gun for a set of operating conditions was characterized by the time-averaged arc voltage and the gas velocity on the jet centerline at the nozzle exit. Relationships between both variables and the working parameters of the torch were established from a dimensional analysis. This method made it possible to deduce the logical dimensionless groups of the variables involved in the process. Such relationships can help (a) to have a better understanding of the effect of the various variables and (b) to predict the variation of arc voltage and gas velocity for a specific plasma gun.

6.1 Dimensional Analysis

In the present study, the variables of the process were the arc current, *I*, in A; the gas flow rate, *G*, in kg/s; and the gas composition for a specific nozzle diameter, *D*, in m. They were collected in the following dimensionless numbers deduced from the physical equations that govern the working of the gun (i.e., energy transfer, conservation of the momentum, Ohm's law):

- the Reynolds number that characterizes the gas flow regime:

$$\mathrm{Re} = \frac{G}{\mu^* \times D} \qquad \text{(Eq 2)}$$

- the energy number (second number of Yas'ko) (Ref 13):

$$Si = \frac{I^2}{\sigma^* \times h^* \times G \times D} \qquad \text{(Eq 3)}$$

- the Prandtl number, which is a measure of the relative effectiveness of momentum and energy transport by diffusion:

$$Pr = \frac{\mu^* \times h^*}{k^* \times T^*} \qquad \text{(Eq 4)}$$

The thermodynamic and transport properties of the gas mixture involved in the dimensionless numbers were calculated at a reference temperature, T^*. The latter is the temperature for which electron concentration in the plasma is higher than 1 vol%.

In Eq 2-4, k^*, μ^*, h^*, and σ^* are the thermal conductivity, the viscosity, the mass enthalpy, and the electrical conductivity, respectively, at T^*. All terms of these numbers were expressed in the SI system.

T^* and the gas properties at T^* were calculated using the ADEP program (Ref 3). Their values are presented in Table 4.

The voltage, *V*, was expressed through a dimensionless number that represents the arc electrical resistance:

$$Su = \frac{V \times D \times \sigma^*}{I} \qquad \text{(Eq 5)}$$

and the maximum gas velocity, v_{max}, was expressed through a dimensionless velocity defined as:

$$P_v = \frac{v_{max}}{V_0} \qquad \text{(Eq 6)}$$

$$\text{where } V_0 = \frac{G}{D^2 \times \rho^*} \qquad \text{(Eq 7)}$$

Here, ρ^* is the specific density of the gas at T^*.

6.2 Arc Voltage

The functional relationships between *Su* and *Pv*, and the dimensionless groups *Re*, *Si*, and *Pr* were determined from a power law expressed as:

$$Su = a \cdot (\mathrm{Re})^b \cdot (Pr)^c \cdot (Si)^d \qquad \text{(Eq 8)}$$

and

$$Pv = a' \cdot (\mathrm{Re})^{b'} \cdot (Pr)^{c'} \cdot (Si)^{d'} \qquad \text{(Eq 9)}$$

where a, b, c, d, a', b', c', and d' are constants. Both equations were expressed in logarithmic form as follows:

$$\ln(Su) = \ln(a) + b \cdot \ln(Re) + c \cdot \ln(Pr) + d \cdot \ln(Si) \qquad \text{(Eq 10)}$$

and

Table 4 Thermodynamic and transport properties of the various gas mixtures at reference temperature, T*

Ar/He/H_2 mixture, vol%	T^*, K	h^*, 10^7 J/kg	σ^*, $10^3\ \Omega^{-1}$/m	μ^*, 10^{-4} kg/m · s	k^*, W/m · K
50/40/10	9500	1.28	1.82	2.57	1.42
50/30/20	9400	1.58	1.65	2.53	1.67
40/50/10	9500	1.53	1.73	2.56	1.62
40/40/20	9400	1.89	1.58	2.5	1.85
30/50/20	9500	2.4	1.61	2.48	2.15
30/45/25	9400	2.61	1.50	2.43	2.18

$$\ln(Pv) = \ln(a') + b' \cdot \ln(Re) + c' \cdot \ln(Pr) + d' \cdot \ln(Si) \quad \text{(Eq 11)}$$

Therefore the experimental data can be plotted in a linear form, Fig. 6 and 7.

The *Su* correlation (Eq 10) was established from 46 experimental data as shown in Fig. 6. The curve fitting by the least-squares technique results in the following correlation with a correlation factor (r^2) equal to 0.96:

$$Su = 5.38 \times Re^{-0.21} \times Pr^{-0.01} \times Si^{-0.58} \quad \text{(Eq 12)}$$

Restating this correlation in terms of the dimensional variables yields:

$$V = 5.38 \times A \times D^{-0.22} \times G^{0.37} \times I^{-0.16} \quad \text{(Eq 13)}$$

with

$$A = (\sigma^*)^{-0.42} \times (h^*)^{0.57} \times (\mu^*)^{0.2} \times (k^* \times T^*)^{0.011} \quad \text{(Eq 14)}$$

This equation shows that the dominant factors on arc voltage for a specific gas mixture are the gas mass flow rate, the nozzle diameter, and to a lesser extent, the arc current.

6.3 Gas Velocity

The radial profiles of gas velocity were measured at 2 mm downstream of the nozzle exit. Each profile was determined from at least 10 measurement points, 0.5 mm apart.

The typical sampling time for velocity measurement, at a given point, was 80 ms. As explained in a previous section, some sets of plasma spraying conditions resulted in an unstable operation mode for the gun. When a change in arc mode occurred between two measurements, the radial distribution of gas velocity was asymmetric.

Therefore, only 42 velocity profiles exhibiting a parabolic form were considered to determine the functional relationship between the velocity and the various factors that influence it.

A good fit of the data, with a correlation factor of 0.86, is obtained with Eq 11 (Fig. 7). Nonetheless, by considering each gas mixture separately, the correlation factor (r^2) is 0.90 for Ar/He/H_2 at 40/50/10 vol%, 0.92 for 50/40/10 vol%, 0.93 for 37/55.6/7.4 vol%, 0.97 for 50/30/20 vol%, and 0.99 for 40/40/20 vol%. This confirms the higher stability of the gun working for a higher percentage of hydrogen:

$$P_v = 13.2 \times Re^{-0.53} \times Pr^{-0.88} \times Si^{0.23} \quad \text{(Eq 15)}$$

In terms of dimensional variables, this equation can be expressed as :

$$v_{max} = 13.2 \times B \times D^{-1.7} \times G^{0.23} \times I^{0.47} \quad \text{(Eq 16)}$$

with

$$B = (\sigma^*)^{-0.24} \times (h^*)^{-1.12} \times (\mu^*)^{-0.35} \times (\rho^*)^{-1} \times (k^* \times T^*)^{0.88} \quad \text{(Eq 17)}$$

The correlation shows the strong influence of the nozzle diameter, *D*, on v_{max}, which varies roughly as the inverse of the nozzle internal cross section surface and is proportional to the arc current, *I*, with the influence of the gas flow rate, *G*, being much smaller.

7. Conclusions

In plasma spraying, the composition of the plasma gas partly controls the operating of the torch and the heating and acceleration of particles injected into the gas flow. The addition of both hydrogen and helium to argon makes it possible to combine the advantages of the high thermal conductivity of hydrogen and high viscosity of helium. This results in an efficient heat transfer to particles and less entrainment of the surrounding atmosphere gas.

In the present study, the arc behavior and the plasma jet were investigated for various Ar-He-H_2 gas mixtures. The arc motion was studied through time-monitoring of arc voltage, and the plasma jet was studied through the measure of gas velocity in the potential core of the jet. Results were expressed in terms of correlations between the average values of voltage and gas velocity, and the variable parameters of this study (i.e., arc current , gas flow rate, and gas composition for a given nozzle diameter).

The results show that the arc voltage is to a great extent controlled by the gas-mass flow rate and composition, and by the nozzle diameter. The gas velocity is mainly influenced by nozzle diameter and arc current, *I*. In addition, for the range of the operating parameters of the plasma gun, two operating modes of the gun were observed: a rather stable mode and a more unstable one. The latter occurred for a low flow rate of argon (between 10 and 13 slm) and high current (460 or 600 A).

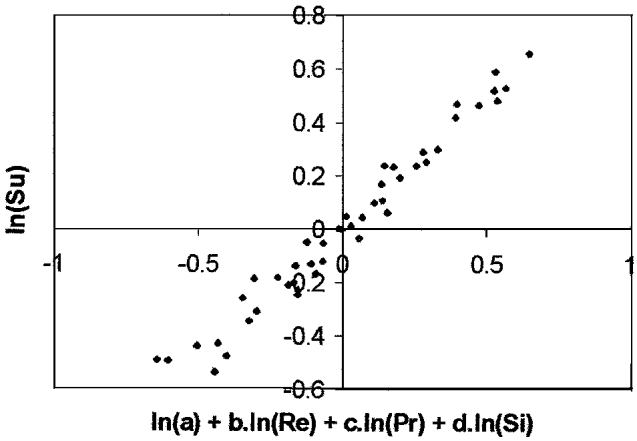

Fig. 6 Correlation between *Su* and the dimensionless numbers *Re*, *Pr*, and *Si*

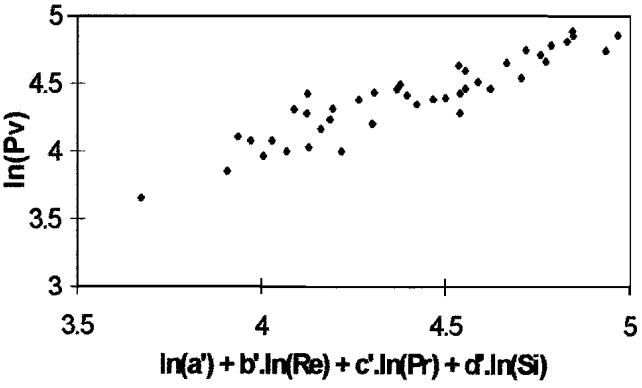

Fig. 7 Velocity correlations with operating parameters

References

1. M.I. Boulos, P. Fauchais, and E. Pfender, *Thermal Plasma: Fundamental and Applications*, Vol 1, Plenum Press, 1994
2. D. Nicoud, J.M. Léger, P. Fauchais, and A. Grimaud, Air Liquide European Patent EP 0451051 A1, 1991
3. B. Pateyron and G. Delluc, ADEP Data Bank of University of Limoges and CNRS, Direction des Bibliothèques, des Musées et de l'Information Scientifique et Technique, 1986
4. A. Vardelle, "Numerical Study of Heat, Momentum and Mass Transfers between an Arc Plasma at Atmospheric Pressure and Solid Particles," master's thesis, University of Limoges-France, No. 29, 1987 (in French)
5. M.P. Planche, P. Fauchais, J.F. Coudert, O. Betoule, and H. Valetoux, Comparison of D.C. Plasma Jet Velocity Distributions for Different Plasma Gas Mixtures: Ar-H_2, Ar-He, Ar-He-H_2, *Proc. of the Seventh National Spray Conf.: Thermal Spray Industrial Applications*, C.C. Berndt and S. Sampath, Ed., ASM International, 1994, p 349-353
6. S.A. Wutzke, E. Pfender, and E.C. Eckert, Study of Electric-Arc Behavior with Superimposed Flow, *AIAA J.*, Vol 5 (No. 4), 1967, p 707-717
7. E. Pfender, J. Fincke, and R. Spores, Entrainment of Cold Gas into Thermal Plasma Jets, *Plasma Chem. Plasma Process.*, Vol 11 (No. 4), 1991, p 529-543
8. M.P. Planche, "Contribution to the Study of a Plasma Gun: Application to the Arc Dynamic and the Measurements of Plasma Flow Velocity," Ph.D. dissertation, University of Limoges-France, No. 37, 1995 (in French)
9. M.P. Planche, J.F. Coudert, and P. Fauchais, Velocity Measurements for Arc Jets Produced by a D.C. Plasma Spray Torch, *Plasma Chem. Plasma Process.*, Vol 18 (No. 2), 1998, p 263-286
10. J.F. Coudert, M.P. Planche, and P. Fauchais, Velocity Measurement of D.C. Plasma Jets Based on Arc Root Fluctuations, *Plasma Chem. Plasma Process.*, Vol 15 (No. 1), 1995, p 47-70
11. A. Vardelle, P. Fauchais, B. Dussoubs, and N.J. Themelis, Heat Generation and Particle Injection in a Thermal Plasma Torch, *Plasma Chem. Plasma Process.*, Vol 18 (No. 4), 1998, p 551-578
12. S.C. Snyder, A.B. Murphy, D.L. Hofeldt, and L.D. Reynolds, Diffusion of Atomic Hydrogen in an Atmospheric Pressure Free-Burning Arc Discharge, *Phys. Rev. E*, Vol 52 (No. 3), 1995, p 2999-3009
13. O.I. Yas'ko, Correlation of the Characteristics of Electric Arcs, *Brit. J. Appl. Phys., Vol 2, 1969, p 733-742*